Cancer Letters 457 (2019) 129–141

Contents lists available at ScienceDirect

Cancer Letters

journal homepage: www.elsevier.com/locate/canlet

Original Articles

Small molecule inhibitor agerafenib effectively suppresses neuroblastoma tumor growth in mouse models via inhibiting ERK MAPK signaling

Hui Li[a,d,1], Yang Yu[a,1], Yanling Zhao[a], Deanna Wu[a], Xiaoman Yu[a], Jiaxiong Lu[a], Zhenghu Chen[b], Huiyuan Zhang[a], Yongguang Hu[a], Yuanfen Zhai[a], Jun Su[a], Ayinuer Aheman[b], Augusto De las Casas[a], Jingling Jin[a], Xin Xu[a], Zhongcheng Shi[c], Sarah E. Woodfield[b], Sanjeev A. Vasudevan[b], Saurabh Agarwal[a], Yusheng Yan[d], Jianhua Yang[a,*], Jennifer H. Foster[a,**]

[a] Texas Children's Cancer Center, Department of Pediatrics, Dan L. Duncan Cancer Center, Baylor College of Medicine, Houston, TX, 77030, USA
[b] Division of Pediatric Surgery, Texas Children's Hospital Department of Surgery, Michael E. DeBakey Department of Surgery, Dan L. Duncan Cancer Center, Baylor College of Medicine, Houston, TX, 77030, USA
[c] Department of Pathology and Immunology, Baylor College of Medicine, Houston, TX, 77030, USA
[d] Department of Cardiothoracic Surgery, Zhujiang Hospital, Southern Medical University, Guangzhou, 510282, PR China

ARTICLE INFO

Keywords:
Neuroblastoma
Agerafenib
RAF
MAPK

ABSTRACT

Neuroblastoma (NB) is the most common extracranial solid tumor in early childhood. Despite intensive multimodal therapy, nearly half of children with high-risk disease will relapse with therapy-resistant tumors. Dysregulation of MAPK pathway has been implicated in the pathogenesis of relapsed and refractory NB patients, which underscores the possibility of targeting MAPK signaling cascade as a novel therapeutic strategy. In this study, we found that high expressions of RAF family kinases correlated with advanced tumor stage, high-risk disease, tumor progression, and poor overall survival. Targeted inhibition of RAF family kinases with the novel small molecule inhibitor agerafenib abrogated the activation of ERK MAPK pathway in NB cells. Agerafenib significantly inhibited the cell proliferation and colony formation ability of NB cells *in vitro*, and its combination with traditional chemotherapy showed a synergistic pro-apoptotic effect. More importantly, agerafenib exhibited a favorable toxicity profile, potently suppressed tumor growth, and prolonged survival in NB mouse models. In conclusion, our preclinical data suggest that agerafenib might be an effective therapeutic agent for NB treatment, both as a single-agent and in combination with chemotherapy.

1. Introduction

Neuroblastoma (NB) is the most common extracranial solid tumor in children, accounting for 7% of all childhood malignancies and 15% of childhood cancer mortality [1–4]. Over the past decade, risk-based stratified treatment resulted in substantial improvement in the outcome for NB [5]. However, despite the intensive treatment, survival for high-risk patients remains low, with approximately half of patients alive at 5 years [6]. Up to 60% of patients relapse with therapy-resistant tumors [7]. Therefore, treatment for high-risk NB remains a challenge, and novel therapeutic approaches are urgently needed.

The mitogen-activated protein kinase (MAPK) pathway is a key driver of oncogenicity in approximately 30% of cancers. This pathway transmits growth and mitogen signals to the nucleus via a cascade of specific phosphorylation events involving RAS, RAF, MEK and ERK [8]. Recent advanced genomic sequencing technology has revealed that 78% of relapsed neuroblastoma samples contain mutations predicted to hyperactivate MAPK signaling [9]. In addition, amplification and activating mutations of receptor tyrosine kinases, such as EGFR, FGFR, ALK and RET, are also frequently implicated in the aberrant activation of the MAPK signaling pathway [10–13]. All of these findings underscore the significance of modulating the MAPK signaling axis for NB treatment.

The RAF family kinases (ARAF, BRAF, and CRAF) constitute core components of MAPK pathway cascade and mediate signals from cell

Abbreviations: NB, neuroblastoma; MAPK, mitogen-activated protein kinase; RAF, rapidly accelerated fibrosarcoma; ERK, extracellular signal–regulated kinases; GDNF, glial cell line-derived neurotrophic factor; EGF, epidermal growth factor; bFGF, basic fibroblast growth factor

* Corresponding author.
** Corresponding author.
E-mail addresses: jianhuay@bcm.edu (J. Yang), jhfoster@bcm.edu (J.H. Foster).

[1] Both authors contributed equally to this work.

https://doi.org/10.1016/j.canlet.2019.05.011
Received 18 November 2018; Received in revised form 2 May 2019; Accepted 8 May 2019

surface receptors to the nucleus, regulating cell growth, differentiation and survival [8,14,15]. Of the known *RAF* genes, *ARAF* mutation is rare in cancers, and is believed to function as a modulator of BRAF function to activate the MAPK pathway [16]. *BRAF* is the most extensively studied and its somatic mutations are found in multiple malignancies including melanoma (50%), papillary thyroid cancer (45%), colon cancer (10%) and non-small cell lung cancer (1%–3%) [17–20]. The V600E mutation accounts for nearly 90% of these mutations [21]. Additionally, overexpression of *CRAF* has also been reported to play a fundamental role in the pathogenesis of many types of cancer [22–28]. Pharmacological inhibition of RAF kinase activity with small molecule inhibitors has achieved great success in preclinical and clinical application [29–31]. However, the role of RAF family kinases in NB pathogenesis and their potential role as a therapeutic target in the treatment of NB is less understood.

To clarify the clinical significance of *RAF* expression in NB, we analyzed RNA-seq data from a large clinical cohort of 498 NB patients and found that higher *RAF* expression (*ARAF, BRAF,* and *CRAF*) correlated with advanced tumor stage, high-risk disease, tumor progression, and poor clinical outcome. We then evaluated the efficacy of inhibiting MAPK signaling pathway in NB cells by a novel small molecular pan-RAF inhibitor, agerafenib (also known as CEP-32496 or RXDX-105). We chose agerafenib for its high binding affinity for both BRAF (mutant and wide-type) and CRAF [32]. Our data showed that agerafenib effectively inhibited ERK MAPK activation. Furthermore, we investigated the therapeutic effect of agerafenib on NB cell lines and animal models. *In vitro*, agerafenib not only inhibited the cell proliferation and colony formation ability in a panel of NB cell lines, it also exerted a synergistic pro-apoptotic effect when combined with chemotherapeutic agent doxorubicin. More importantly, agerafenib potently suppressed tumor growth and prolonged animal survival in mouse models, exhibiting a robust *in vivo* anti-tumor activity. In conclusion, our preclinical data suggest that agerafenib is a promising therapeutic agent for high-risk or relapsed NB patients, as a single-agent treatment or in combination with chemotherapy.

2. Materials and methods

2.1. Cell lines and cell culture

Three *MYCN*-amplified (NGP, IMR-32, SK-N-BE(2)) and three *MYCN*-non-amplified cell lines (SH-SY5Y, SK-N-AS and LAN-6) were maintained in RPMI-1640 medium (Lonza, Walkersville, MD, USA), supplemented with 20% (v/v) heat inactivated fetal bovine serum (FBS) (SAFC Biosciences, Lenexa, KS, USA), 100 units/ml penicillin, and 100 μg/ml streptomycin at 37 °C in 5% CO_2. The NGP-luciferase cell line was generated by transfection with a pcDNA3 luciferase expression plasmid into the NGP cells as described previously [33,34]. All cell lines were obtained between 2005 and 2017, and authenticated via short tandem repeat (STR) analysis in MD Anderson Cancer Center. Mycoplasma testing was performed by LookOut® Mycoplasma PCR Detection Kit (MP0035, Sigma-Aldrich).

2.2. Clinical patient cohort

The tumor neuroblastoma dataset SEGC (N = 498, GSE62564) and the Kocak neuroblastoma patient dataset (N = 649, GSE45547, probe set: ag44kcwolf) that includes RNA-seq and microarray profiles of unique primary tumors are publicly available in the R2: Genomic Analysis and Visualization Platform database (http://hgserver1.amc.nl/cgibin/r2/main.cgi).

2.3. Antibodies and reagents

Agerafenib (#HY-15200), trametinib (#HY-10999), and vemurafenib (#HY-12057) were purchased from MedChem Express (Monmouth Junction, NJ, USA). Recombinant human EGF (#236-EG), bFGF (#233-FB), and GDNF (#212-GD) were purchased from R&D systems (Minneapolis, MN, USA). Anti-β-actin (#A2228) antibody was purchased from Sigma (St. Louis, MO, USA). The phospho-mTOR (S2448; #5536), mTOR (#2792), phospho-STAT3 (T705; #9145), STAT3 (#12640), phospho-ERK (T202/Y204; #9106L), ERK1/2 (#9102L), phospho-AKT (S473; #4060S), AKT (#9272S), phospho-S6 (S235/S236; #4858S), S6(#2217S), PARP (#9542L), Cleaved Caspase-3 (A175; #9664S) antibodies and anti-rabbit (#7074S) and anti-mouse (#7076S) secondary antibodies were purchased from Cell Signaling Technology (Danvers, MA, USA). For the immunohistochemical assay, the DAKO Envision System (DAKO Co., Carpinteria, CA, USA) was employed. Monoclonal anti-mouse Ki67 (#NB110-89717APC) were purchased from Novus Biologicals (Littleton, CO, USA). Monoclonal mouse anti-human Ki67 (#558615) was purchased from BD Pharmingen (San Diego, CA, USA). Cleaved Caspase-3 (A175; #9664S) were purchased from Cell Signaling Technology (Danvers, MA, USA).

2.4. Cell proliferation assay

NB cells were seeded in 96-well plates at the concentration of 5×10^3 cells per well. Sixteen hours later, the media were changed and cells were treated with 0 μM, 0.25 μM, 0.5 μM, 1 μM, 2 μM, 4 μM, 8 μM, 16 μM, 32 μM, or 64 μM of agerafenib for 72 h. Cell proliferation was measured by Cell Counting kit-8 (Dojindo Molecular Technologies Inc., Rockville, MD, USA) following the manufacturer's instructions. For trametinib and vemurafenib treatment, NB cells were seeded at the same concentration with agerafenib, then were incubated with 0 μM, 0.25 μM, 1 μM, 4 μM, 16 μM, or 64 μM of trametinib or vemurafenib for 72 h. Cell proliferation was measured by MTT assay (Sigma, St. Louis, USA) following the manufacturer's instructions. Each result was performed in six replicates.

2.5. Cell imaging

NB cells were seeded in 96-well plates at a concentration of 5×10^3 cells per well. Sixteen hours later, cells were treated with 0 μM, 0.5 μM, or 8 μM of agerafenib or equal volumes of DMSO. Cell morphologies were observed and captured using an optical microscope after 72 h of treatment. Each result was performed in triplicate.

2.6. Immunoblotting

Cell lysates were obtained by washing the cells in culture dishes twice with ice cold PBS and then scrapping into RIPA lysis buffer (25 mM HEPES (PH7.7), 135 mM NaCl, 1% Triton X-100, 25 mM β-glycerophosphate, 0.1 mM sodium orthovanadate, 0.5 mM phenylmethylsulfonyl fluoride, 1 mM dithiothreitol, 10 μg/mL aprotinin, 10 μg/mL leupeptin, 1 mM Benzamidine, 20 mM disodium β-nitrophenylphosphate, and phosphatase inhibitor cocktail 2 and 3 (#P5726 and #P0044, Sigma)). After centrifuging at 13,000 × g for 15 min at 4 °C, supernatants were collected, resolved by SDS polyacrylamide gel electrophoresis (PAGE) and transferred to PVDF membranes. The membranes were probed with corresponding primary antibodies overnight at 4 °C and the IgG horseradish peroxidase-conjugated secondary antibodies against mouse or rabbit for 1 h at room temperature (25 °C). The proteins were detected by using the ECL-Plus Western blotting detection system (GE Health).

2.7. Anchorage-independent cell proliferation assay

The soft agar assay was performed as described previously [35]. Briefly, a 5% (w/v) base agar was made by adding noble agar (Difco Laboratories, Detroit, MI, USA) into distilled water, and then the mixture was autoclaved for 50 min followed by cooling to 56 °C in a water bath. A 0.5% bottom gel (mixture of base agar, RPMI-1640 containing

10% FBS) was plated in 12-well plates (1.0 mL per well) then cooled until semi-solid. For the top agar layer, each NB cell line was counted and added to 1.0 ml 0.3% agar at 3×10^3 cells/well along with 0 μM, 2 μM, or 4 μM of agerafenib. Cells grew at 37 °C in 5% CO_2 for 2 weeks, then were stained with 500 μL of 0.5% (w/v) MTT solution. Images were captured and colonies were counted by VersaDoc Imaging System (Bio-Rad, CA, USA) after 4 h. Each assay was performed in triplicate.

2.8. Synergy studies

NB cells (SK–N-BE(2), SK-N-AS) were seeded in 96-well plates at the concentration of 1×10^4 cells per well. Sixteen hours later, the media were changed. Combination index (CI) studies were performed by treating cells with agerafenib, doxorubicin, or their combination. The CI values and dose-reduction indices (DRIs) were calculated by the Chou-Talalay method for drug interactions using Compusyn software for the different fractions affected [36]. CI < 1, $= 1$, and > 1 indicates synergism, additive effect and antagonism, respectively. DRI > 1, and < 1 indicates a favorable and an unfavorable dose reduction, respectively.

2.9. Flow cytometric analysis of apoptosis

The PE Annexin V Apoptosis Detection Kit I (#559763, BD Biosciences) was used to determine cellular apoptosis. Cells were plated at 1.5×10^6 cells in 6-cm plates and treated the following day after incubation with either doxorubicin, agerafenib, or their combinations for 24 h at 37 °C. Cells were then harvested, resuspended in Annexin V binding buffer, and stained with Annexin V and 7-amino-actinomyosin D (7-AAD) according to the manufacturer's instructions. The resulting percentage apoptosis for each cell line was analyzed using a Cytomics™ FC500 flow cytometer (Beckman Coulter, Inc., Brea, CA, USA) and disposed with FlowJo 7.6.5. (FlowJo, LLC, Ashland, OR, USA).

2.10. Xenograft NB mouse model

The most common tumor-bearing sites of NB are adrenal gland, retroperitoneum, thorax, pelvis and neck. Among all of the sites to develop a clinically relevant *in vivo* xenograft tumor model, adrenal gland is the ideal one because NB most commonly arises in and around the adrenal glands. However, injection of NB cells into the adrenal gland is technically challenging due to small size of the mouse adrenal gland. Therefore, many studies used the kidney capsule as an alternative injection site to establish xenograft NB mouse model [37].

Five to six-week-old female athymic (*nu/nu*) mice were purchased from Taconic Biosciences (Hudson, NY, USA) and maintained under barrier conditions. Subconfluent luciferase-transduced NGP cells were harvested and kept on ice until xenotransplantation. The recipient mice were shaved and sterilized with 70% ethanol at the site of incision and anesthetized. An inoculum of 1×10^6 prepared NGP cells in 0.1 ml of PBS was injected into the left renal capsule through a left flank incision with a 25-gauge needle, which was closed with a single 4-0 suture (Polysorb, US Surgical, Norwalk, CT, USA) and staples in 2 layers. All handling of the animals was performed under aseptic conditions. Two weeks after xenografting, mice bearing tumors with similar sizes (using bioluminescent imaging to monitor tumor growth) were randomly divided into two groups: DMSO control group and agerafenib treatment group (30 mg/kg by intraperitoneal (i.p.) injection once daily for 21 days). Both control and treatment groups included 4 mice. At the end of the treatment, all mice were sacrificed. Tumors, together with the right kidneys (control), were harvested, weighed, photographed and lysed for western blotting. All animal experiments were performed according to procedures approved by Institutional Animal Care and Use Committee of Baylor College of Medicine.

2.11. TH-MYCN transgenic NB mouse model

The generation and identification of the human *MYCN* transgenic mouse model of neuroblastoma has been previously described [35]. At four weeks of age, following the development of an abdominal tumor (~1 mm in diameter), these TH-*MYCN* transgenic mice were treated daily for 3 consecutive weeks with single intraperitoneal (i.p.) injections of agerafenib at 30 mg/kg or an equal volume of DMSO (controls). Three weeks later, the treatment was stopped and mice were monitored daily for symptoms. Kaplan-Meier survival data were analyzed using a logrank test. All experimental procedures involving mice met the required standards and were approved by the Institutional Animal Care and Use Committee of the Baylor College of Medicine.

2.12. Immunohistochemistry

Paraffin embedded tumor sections from both xenograft and TH-*MYCN* transgenic NB mouse models were washed twice in fresh xylene for 5 min each to remove paraffin. The slides were rehydrated through a series of graded ethanol, and finally in distilled water for 5 min. Endogenous peroxidase activity was blocked using 3% hydrogen peroxide for 10 min at RT and non-specific binding was blocked with Odyssey Blocking Buffer (LI-COR Biosciences, Lincoln, NE, USA). After antigen retrieval, tissue sections were incubated with anti-cleaved caspase-3 for 16 h at 4 °C and visualized using the DAKO EnVision™ Kit (Dako, Carpinteria, CA, USA). For Ki67 detection, tissue sections from TH-*MYCN* transgenic mouse model were incubated with rabbit anti-Ki67 mouse specific antibody for 16 h at 4 °C, followed by washing in TBS-0.1% Tween-20, and visualized as above. Tissue sections from both xenograft and *TH-MYCN* transgenic NB mouse model were incubated with rabbit anti-Ki67 human specific antibody for 16 h at 4 °C, followed by washing in TBS-0.1% Tween-20, and visualized as above. For quantitative analyses of Ki67 and cleaved caspase-3 staining, tumor section slides from both xenograft and TH-*MYCN* transgenic NB mouse models were examined with a light microscope coupled to a digital camera system (Axiocam HRP, Zeiss, Germany) at a final magnification of 40 × . For each case a minimum of 1000 nuclei located in the basal and suprabasal layers were counted in up to 20 consecutive microscopic fields per case.

2.13. Statistical analysis

A two-tailed Student's *t*-test was used to determine the statistical significance of *in vitro* and *in vivo* assay between the control and agerafenib treatment groups. Each assay was repeated at least twice, and representative results were presented. All values were presented as mean ± standard deviation (SD). A value of $P < 0.05$ was taken to indicate statistical significance.

3. Results

3.1. High expression of RAF genes was associated with poor prognosis in NB patients

To clarify the clinical significance of *RAF* expression in NB, we evaluated RNA-seq data from a large clinical cohort of patients (http://r2.amc.nl)). Kaplan-Meier analysis from the Tumor Neuroblastoma SEQC dataset, GSE49710, (n = 498) revealed that all of the three *RAF* gene expressions were inversely associated with overall and event-free survival in NB (Fig. 1A and B), with a higher expression level in patients with stage 4 disease (International Neuroblastoma Staging System Committee (INSS) stages) (Fig. 1C). Moreover, high expression of *RAF* genes was associated with high risk disease and tumor progression (Fig. 1D and E). To confirm our finding, we analyzed another dataset of 649 patients (GSE45547, Kocak-649-cohort) and obtained similar results (Fig.S1). These data suggest that RAF family kinases play an

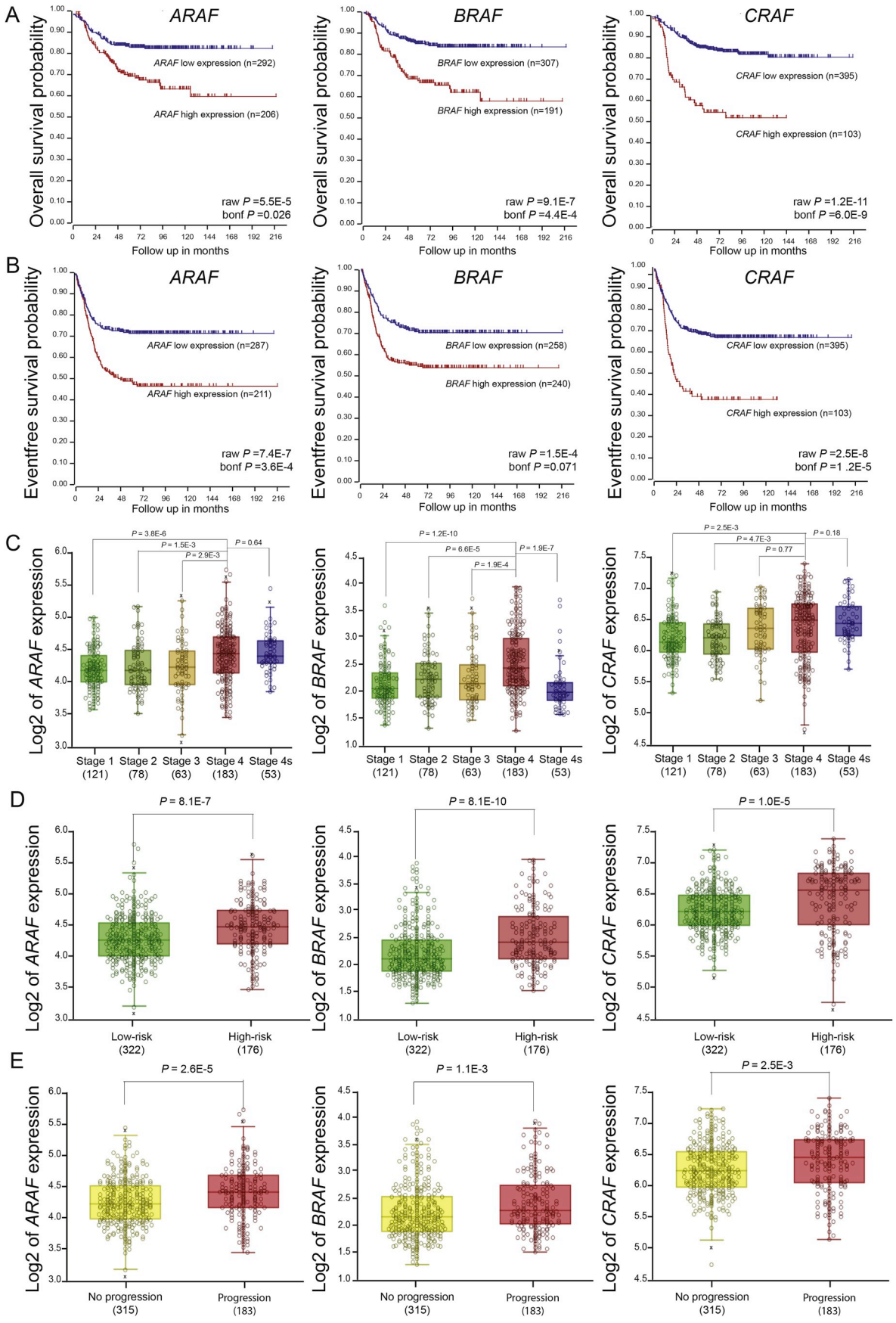

(caption on next page)

Fig. 1. High expression of *RAF* genes is associated with poor prognosis in NB. A large cohort of NB patient RNA-seq dataset (R2: Genomics Analysis and Visualization Platform (http://r2.amc.nl)) with annotated clinical and long-term follow-up data was used to analyze the outcomes in patients with NB. (A, B) Kaplan-Meier curves show the probability of overall survival (A) and event-free survival (B) based on *RAF* (*ARAF, BRAF,* and *CRAF*) gene expression (P values were calculated by Student *t*-test). (C, D, E) R2 dataset shows high expression level of each *RAF* family gene in stage 4 group compared with other groups (C) and a significant correlation of high expression level of each *RAF* gene with high-risk disease (D) and tumor progression (E).

Table 1
Gene amplification and mutation status in six neuroblastoma cell lines.

Cell lines	MYCN genomic amplification	RAS	TP53
IMR-32	Amplified	Wild-type	Wild-type
NGP	Amplified	Wild-type	Wild-type
SK-N-BE2	Amplified	Wild-type	Mutant
SH-SY5Y	Non-amplified	Wild-type	Wild-type
SK-N-AS	Non-amplified	NRAS	Mutant
LAN-6	Non-amplified	KRAS	Wild-type

important role in the pathogenesis and tumor progression of NB.

3.2. Small molecular inhibitor agerafenib abrogates ERK MAPK signaling pathway in NB cells

With the demonstrated significance of *RAF* overexpression in high-risk NB, we hypothesized that inhibiting RAF kinases with agerafenib would abrogate MAPK signaling pathway activation in NB. Genomic amplification of *MYCN* is observed in 20%–25% of all NB patients and is considered to be a hallmark for high-risk disease [38]. To clarify whether *MYCN* status may influence the inhibitory effect of agerafenib, we selected a panel of six NB cell lines (Table 1), in which three were *MYCN*-amplified cell (NGP, IMR-32, and SK-N-BE(2)) and three were *MYCN*-non-amplified cell (SH-SY5Y, SK-N-AS, and LAN-6). Previous studies shows that besides the RAF oncogeic pathway, agerafenib also blocks signaling pathways such as PI3K/AKT/mTOR and JAK/STAT to suppress tumor cell proliferation [31]. We examined the effect of agerafenib on these pathways in NB by detecting the protein levels of phospho-AKT, phospho-mTOR, phospho-STAT3, phospho-ERK (T204/Y204), and phosphor-S6 (S235/S236) in the *MYCN*-amplified cell line NGP and the *MYCN*-non-amplified cell line SH-SY5Y after treatment with agerafenib (Fig.S2A). We found that agerafenib has no effect on phospho-AKT, phospho-mTOR, and phospho-STAT3 levels in both cell lines. However, the decreased phospho-ERK and phospho-S6 levels were detected after agerafenib treatment in a dose-dependent manner (Fig.S2A). To further confirm the result, we examined phosphorylated ERK (T204/Y204) and S6 (S235/S236) protein levels in other four NB cell lines incubated with a series of concentrations of agerafenib. A dramatic reduction of the phosphorylated ERK (T204/Y204) and S6 (S235/S236) was noticed in NGP, SK-N-BE(2), and LAN-6 upon 1 μM of agerafenib treatment, while the level of ERK phosphorylation was largely unchanged for doses up to 4 μM in SK-N-AS (Fig. 2A). Furthermore, in order to reveal the early change of MAPK signaling cascade after agerafenib treatment, four NB cell lines (NGP, LAN-6, SK-N-BE(2), and SK-N-AS) were treated with indicated doses of agerafenib for varying length of time (0 ~ 8 h). Similar to the effect after 24 h of treatment, 10 μM of agerafenib significantly inhibited the phosphorylation of ERK (T204/Y204) and S6 (S235/S236) in all of the cell lines tested after 8 h of treatment (Fig. 2B). We also found that low concentrations of agerafenib treatment (2 μM, 4 μM, and 6 μM) could achieve partial blockage of the MAPK signaling pathway in the short time period treatment (< 8 h) (Fig.S2B). These data indicate that agerafenib could inhibit the ERK MAPK signaling pathway in all of the cell lines tested, irrespective of *MYCN* status.

3.3. Agerafenib effectively inhibits multiple growth factors-induced ERK MAPK activation

Growth factors play an important role in tumorigenesis and tumor progression, and growth factor-induced intracellular signaling also completely or partly converge on the MAPK cascade. With the inhibitory effect of agerafenib on ERK MAPK signaling observed in NB cells, we tested whether agerafenib could block extracellular growth factors (GDNF, EGF and bFGF)-induced MAPK activation. GDNF, EGF and bFGF have been shown to be critical for NB survival. As shown in Fig. 2C and Fig.S2C, agerafenib dramatically inhibited growth factor-induced phosphorylation of ERK and S6 in NB cell lines in a dose dependent manner.

3.4. Agerafenib suppresses NB cell proliferation in vitro

To determine the therapeutic effect of agerafenib in preclinical NB cell line models, six NB cell lines including three *MYCN*-amplified cell lines (NGP, IMR-32, and SK-N-BE(2)) and three *MYCN*-non-amplified cell lines (SH-SY5Y, SK-N-AS, and LAN-6) were treated with increasing concentrations of agerafenib for 72 h, then subjected to CCK-8 assay. Our results showed that agerafenib significantly suppressed the cell proliferation in all cell lines tested in a dose-dependent manner (Fig. 3A). The median IC_{50} values of agerafenib on these cell lines ranged from 2.06 μM to 18.4 μM (Fig. 3B). There was an 8.9-fold difference between the most sensitive cell (LAN-6) and the least sensitive cell (SK–N-AS). The IC_{50} values of the tested cell lines were largely consistent with the phosphorylated ERK changes in the previous immunoblotting assay, in which a significant drop of the phosphorylated ERK (T204/Y204) was noticed in NGP, SK-N-BE(2), and LAN-6. In the less sensitive cell line (SK–N-AS), the phosphorylated level of ERK remained unchanged until doses beyond 4 μM. The *RAS* gene profile and sensitivity of these cell lines to agerafenib had no significant correlation with the *MYCN* or *TP53* status. Two *RAS* mutant cell lines in our experiment, LAN-6 ($KRAS^{G12C}$) and SK-N-AS ($NRAS^{Q61K}$), showed different responses to agerafenib, the former being sensitive with the lowest IC_{50} value and the latter being resistant with the highest IC_{50} value. Besides the CCK-8 assay, the inhibitory effect of agerafenib on NB cell proliferation was also confirmed by examining the cell morphological changes after treatment (Fig. 3C). The colony-formation capacity of the six cell lines after 24-h agerafenib treatment was also significantly suppressed in a dose-dependent manner (Fig.S3A). For better evaluation of the therapeutic effect of agerafenib, we also examined the effect of two other MAPK signaling inhibitors, vemurafenib and trametinib, on NB cell proliferation. Wefound that the average IC_{50} value of vemurafenib was over 25 μM and the IC_{50} values of trametinib ranged from 13.21 μM to 18.4 μM, with the exception of SK-N-AS, which was highly sensitive to trametinib (IC_{50} = 80 nM) (Fig. S3B-S3E).

3.5. Agerafenib suppresses anchorage-independent growth of NB cells

Anchorage-independent growth in soft agar is a characteristic of highly malignant cancer cells. To investigate the effects of agerafenib on anchorage-independent colony formation and growth, we performed soft agar assays in four NB cell lines including two *MYCN*-amplified cell lines (NGP and SK-N-BE(2)) and two *MYCN*-non-amplified cell lines (SH-SY5Y and SK-N-AS). Compared with the control group, treatment

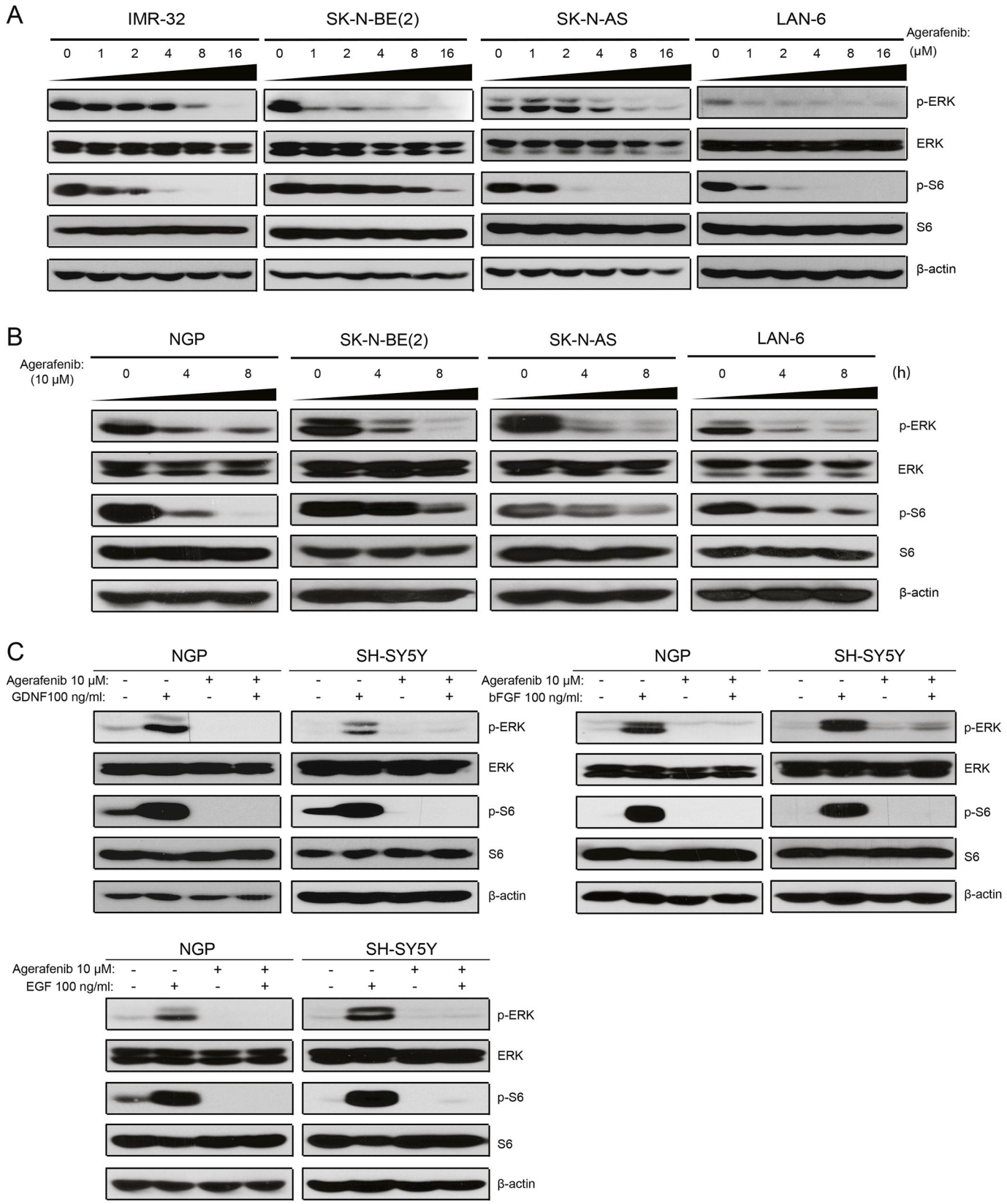

Fig. 2. Small molecular inhibitor agerafenib suppresses ERK MAPK activation in NB cells. **(A)** Four NB cell lines, IMR-32, SK-N-BE(2), SK-N-AS and LAN-6 were treated with increasing concentration of agerafenib for 24 h, then subjected to SDS-PAGE, and immunoblotted with the antibodies indicated. β-actin was used as a loading control for whole cell extracts in all samples. (B) Four NB cell lines (NGP, LAN-6, SK-N-BE(2), and SK-N-AS) were treated with indicated doses of agerafenib for varying length of time (0 h, 4 h, and 8 h), then subjected to SDS-PAGE, and immunoblotted with the antibodies indicated. (C) NGP and SH-SY5Y cell lines were starved in serum-free medium for 16 h before being exposed to agerafenib for 2 h and subsequently stimulated with the indicated dose of GDNF, bFGF, and EGF ligand respectively for varying length of time (GDNF, 10 min; bFGF, 10 min; EGF, 5 min). Then cell lysates were subjected to SDS-PAGE, and immunoblotted with the antibodies indicated.

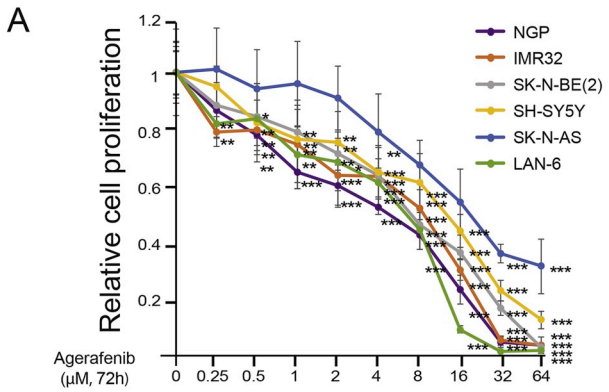

B

IC50 of Agerafenib on NB cell lines

	Cell Lines	IC50 (μM)
MYCN amplified	NGP	2.075
	IMR-32	2.167
	SK-N-BE(2)	3.603
MYCN non-amplified	SH-SY5Y	6.521
	SK-N-AS	18.407
	LAN-6	2.06

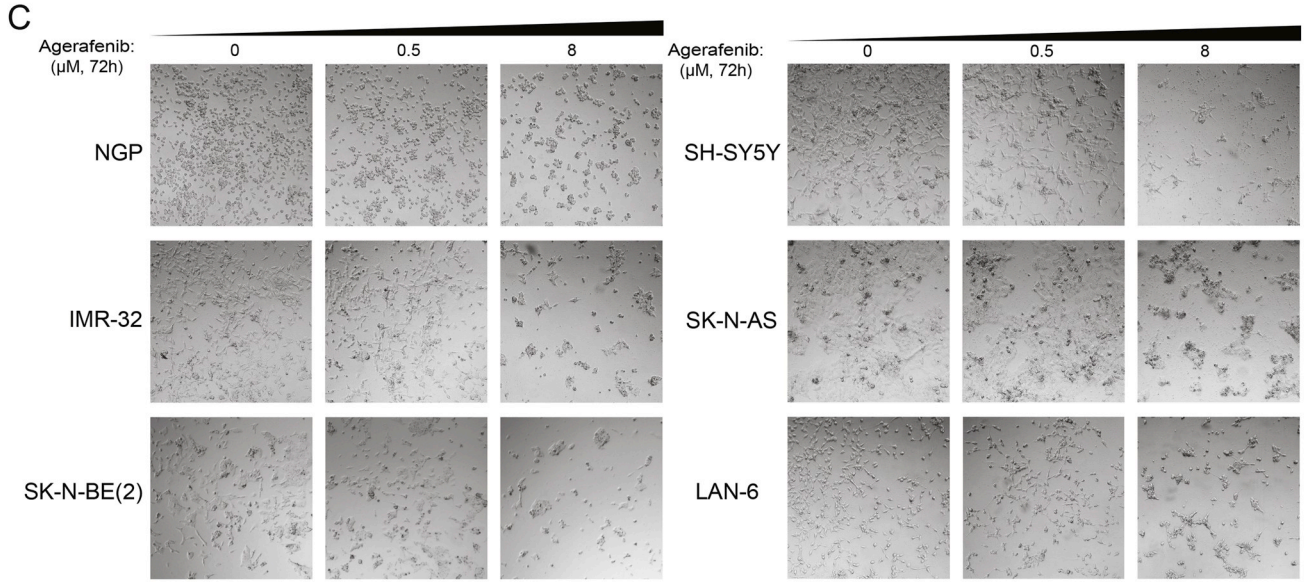

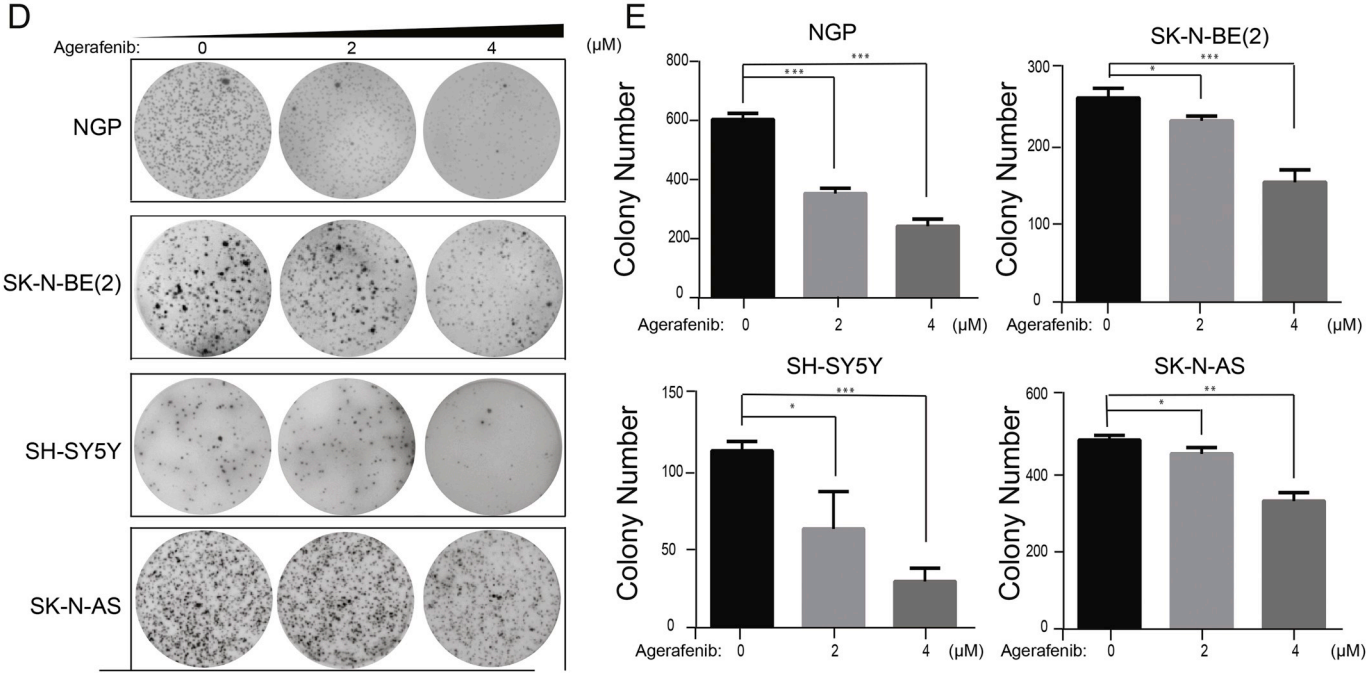

Fig. 3. Agerafenib inhibits NB cell proliferation and anchorage-independent growth *in vitro*. (A) Six NB cell lines (NGP, IMR-32, SK-N-BE(2), SH-SY5Y, SK-N-AS and LAN-6) were treated with the indicated concentrations of agerafenib for 72 h. Cell proliferation was assessed by CCK-8 assays after 72 h of treatment. Data was represented as % vehicle ± S.D. *, $P < 0.05$; **, $P < 0.01$; ***, $P < 0.001$ (Student's *t*-test, two-tailed). (B) List of IC_{50} values of agerafenib on NB cell lines. IC_{50} values were calculated based on the data collected in the CCK-8 assay. (C) Morphological changes of six different NB cell lines treated with increasing concentrations (0 μM, 0.5 μM, 8 μM) of agerafenib for 72 h. (D) The effect of agerafenib on the anchorage-independent cell proliferation. A panel of four NB cell lines were grown in soft agar with 0 μM, 2 μM, or 4 μM of agerafenib for 2 weeks. Cells were stained with 0.5% (w/v) MTT solution to visualize colonies and photographed. (E) Colonies from (D) were counted and colony numbers were represented as % vehicle ± S.D. *, $P < 0.05$; **, $P < 0.01$; ***, $P < 0.001$ (Student's *t*-test, two-tailed).

A

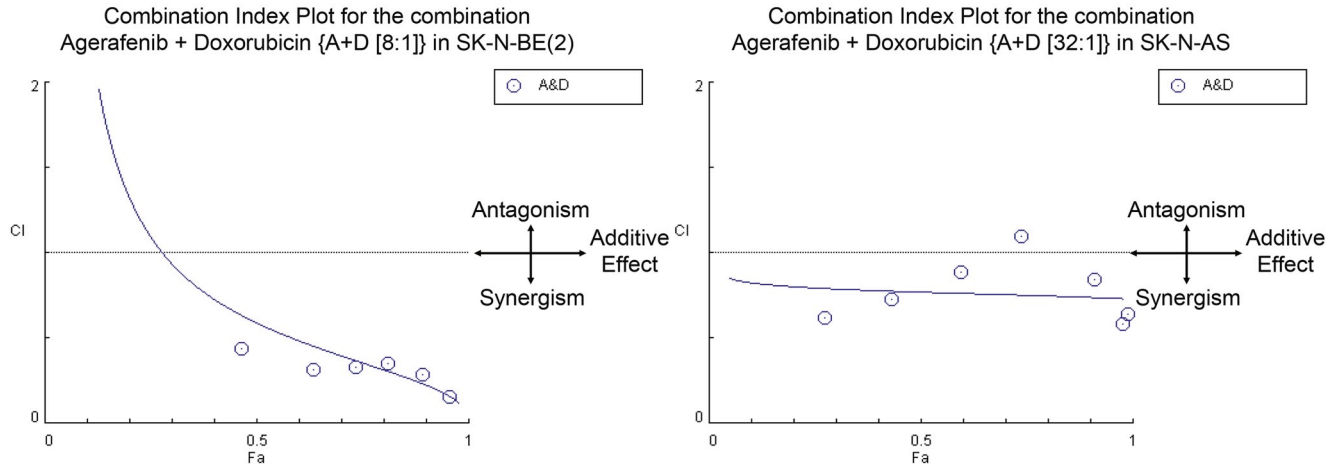

B

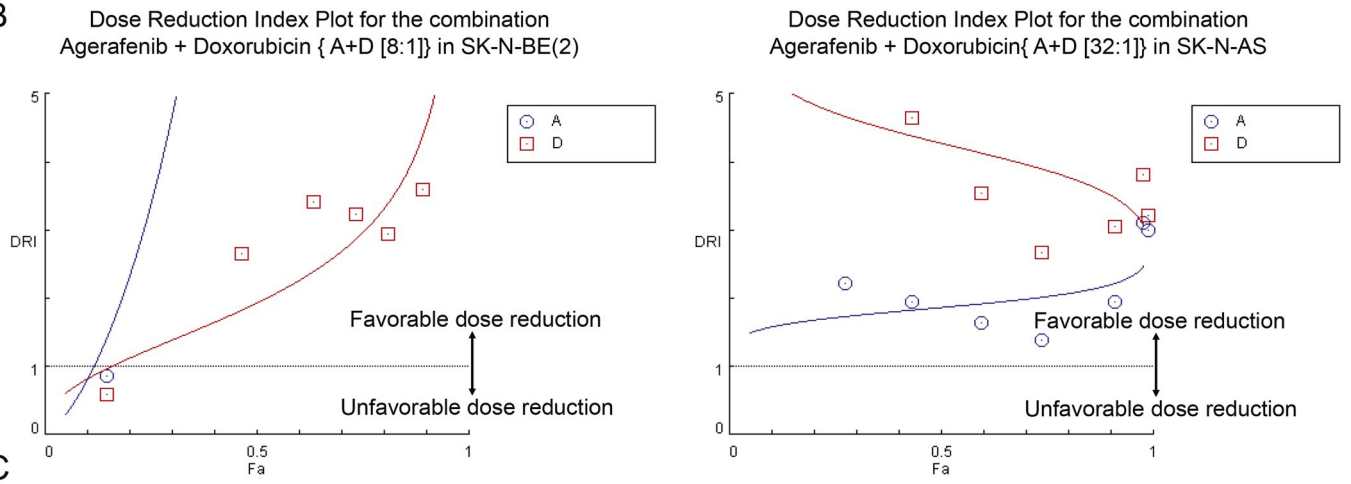

C

Combination Index (CI) values in SK-N-BE(2)				
Combination	ED50	ED75	ED90	ED95
A+D	0.58878	0.35421	0.22360	0.16550

Combination Index (CI) values in SK-N-AS				
Combination	ED50	ED75	ED90	ED95
A+D	0.77014	0.75180	0.73935	0.73425

D

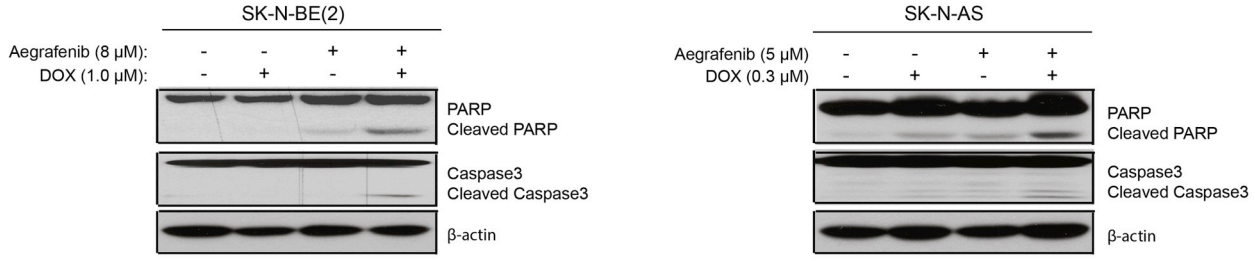

E

SK-N-BE(2)	Live cell (%)	Apoptotic cell (%)
Blank	92.5%	7.5%
Doxorubicin	80.9%	19.1%
Agerafenib	76.6%	23.4%
D + A	52.3%	47.7%

SK-N-AS	Live cell (%)	Apoptotic cell (%)
Blank	89.3%	10.7%
Doxorubicin	69.7%	30.3%
Agerafenib	76.1%	23.9%
D + A	36.6%	63.4%

(caption on next page)

Fig. 4. Agerafenib synergistically enhances the cytotoxic effect of doxorubicin on the chemo-resistant NB cell lines. Combination index (CI) studies were performed by treating SK-N-BE(2) and SK-N-AS cells seeded in 96-well plate with agerafenib, doxorubicin and their combinations at a ratio of 8:1 and 32:1 respectively for 24 h. These CI values were calculated by the Chou-Talalay method for drug interactions using Compusyn software for the different fractions affected. Values of CI < 1, = 1 and > 1 indicate synergism, additive effects and antagonism, respectively. (A) CI plots for SK-N-BE(2) and SK-N-AS. (B) Dose-reduction indices (DRIs) plots were calculated. (DRI > 1 indicates a favorable dose reduction, while a DRI < 1 indicates an unfavorable dose reduction). (C) The obtained CI values for the combination agerafenib and doxorubicin at different effective doses (ED50, ED75, ED90, ED95). (D) SK-N-BE(2) and SK-N-AS were seed in culture dishes and treated with either doxorubicin alone, agerafenib alone, or their combinations for 24 h. Then whole cell lysates were subjected to SDS-PAGE and immunoblotted with the PARP and Caspase 3 antibodies. β-actin was used as a loading control in all samples. (E) Annexin V and 7-AAD cytofluorometric staining was utilized to detect apoptotic SK-N-BE(2) and SK-N-AS cells after treatment with doxorubicin, agerafenib, and their combination for 24 h. The quantification of the apoptotic and live cells were measured and listed (E).

with agerafenib resulted in significantly attenuated anchorage-independent growth in all of these cell lines at the indicated concentrations (0.5 μM, 2 μM, 4 μM) (Fig. 3D and E).

3.6. Agerafenib enhances doxorubicin-induced cytotoxicity in chemo-resistant NB cell lines

Since agerafenib can dramatically suppress the proliferation and anchorage-independent growth in NB cells, we hypothesized that agerafenib may have a synergistic pro-apoptotic effect when combined with a chemotherapeutic agent doxorubicin. To test this hypothesis, we examined the synergistic effect of agerafenib and doxorubicin on two chemo-resistant NB cell lines, SK-N-BE(2) and SK-N-AS. CI plots showed high and strong synergism of these two agents in SK-N-BE(2) (CI < 0.7 at ED_{50} and ED_{75}, CI < 0.3 at ED_{90} and ED_{95}, respectively) and moderate synergism of these two agents in SK-N-AS (CI = 0.7–0.85 at ED_{50}, ED_{75}, ED_{90} and ED_{95}, respectively) (Fig. 4A). Dose-reduction indices (DRIs) plots indicated a favorable dose reduction after combining agerafenib with doxorubicin (DRI > 1 indicates favorable dose-reduction) (Fig. 4B). The obtained CI values for the combination at different effective doses (ED_{50}, ED_{75}, ED_{90}, and ED_{95}) were also listed (Fig. 4C). After incubation with either doxorubicin, agerafenib, or their combinations for 24 h, apoptosis in SK-N-BE(2) and SK-N-AS were examined by immunoblotting analysis of cleaved caspase-3 and cleaved PARP proteins. Our data revealed an enhanced pro-apoptotic effect when cells were treated by the combination of agerafenib and doxorubicin compared to single-agent (Fig. 4D). To further confirm the pro-apoptotic effect of agerafenib in combination with doxorubinci on NB cells**,** Annexin V-PE/7-AAD flow cytometry analysis was utilized in SK-N-BE(2) and SK-N-AS cells. As shown in Fig. 4E, compared with single treatment groups, there were marked increases in the proportions of apoptotic cells when the two NB cell lines were treated with the combination of doxorubicin and agerafenib (P < 0.01). Taken together, these data suggest that agerafenib combined with conventional chemotherapy may serve as a promising therapeutic strategy for chemo-resistant NB treatment.

3.7. Agerafenib inhibits tumor growth in a xenograft NB mouse model

To better evaluate the *in vivo* therapeutic effect of agerafenib, we established a xenograft model by injecting *MYCN*-amplified NGP cells into the exposed renal capsules of immunocompromised mice. Two weeks after injection, mice with similar size of tumors were randomly divided into two groups and treated with either agerafenib (30 mg/kg) or an equal volume of dimethylsulfoxide (DMSO) by intraperitoneal (i.p.) daily for 21 days as shown (Fig. 5A). Agerafenib treatment was well tolerated without obvious body weight loss and other adverse effect. Agerafenib significantly inhibited tumor growth compared to the control group (Fig. 5B and C). The average tumor weight in the placebo group was 1.01 g (± 0.55 g), whereas the average tumor weight in the treatment group was 0.38 g (± 0.38 g) (P < 0.05). Furthermore, agerafenib effectively inhibited the phosphorylation of ERK (T202/Y204) and S6 (S235/S236) in the tumors from the xenograft models (Fig. 5D). Immunohistochemistry (IHC) staining with cleaved caspases-3 and Ki67 antibody also confirmed the pro-apoptotic and anti-proliferative effect of agerafenib (Fig. 5E). The average number of caspase-3 positive staining cells per field increased from 18.7 (± 4.5) to 30.2 (± 4.8) after agerafenib treatment (P < 0.01) and the number of ki67 positive cells dropped from 33.2 (± 11.0) to 18.5 (± 5.2) (P < 0.01) (Fig. 5F). These data indicate that agerafenib suppresses the ERK MAPK signaling activation in tumors and inhibit the tumor growth.

3.8. Agerafenib prolongs survival in a TH-MYCN transgenic NB mouse model

To further evaluate the *in vivo* anti-tumor effect of agerafenib, we utilized an immunocompetent TH-*MYCN* transgenic NB mouse model, which shares histological and genomic features with human NB. After genotyping confirmation, six four-week-old homozygous TH-*MYCN* transgenic mice were randomly assigned into two groups, and agerafenib was administered by intraperitoneal (i.p.) daily for 21 days as shown (Fig. 5G). The lifespan of the agerafenib-treated TH-*MYCN* transgenic NB mice, when compared to that of the control mice, was prolonged by approximately 10 weeks (Fig. 5H) (logrank, $\chi 2 = 5.213$; P < 0.05). In another set of TH-MYCN transgenic mouse experiment, seven-week-old homozygous mice were treated with either agerafenib or DMSO via i.p. injection daily for two days. IHC staining with cleaved caspases-3 and Ki67 antibody was performed to validate the inhibition of agerafenib on tumor growth (Fig. 5I). Our results showed that agerafenib suppressed tumor cell proliferation (98.9 *vs* 76.9, P < 0.01) and significantly induced apoptosis (32.5 *vs* 56.25, P < 0.01) (Fig. 5J).

4. Discussion

In this study, we verified the clinical significance of RAF family kinases, the key components of MAPK signaling, in the pathogenesis of NB and tested the possibility of pharmacologically modulating the MAPK signaling axis with a RAF inhibitor. The MAPK pathway, also known as the RAS-ERK signaling pathway, is the most frequently dysregulated signaling cascade in many cancer types and is involved in various cellular processes including tumor initiation, maintenance, and therapeutic resistance [39]. Nearly 80% of relapsed neuroblastoma contains mutations predicted to activate the RAS-MAPK pathway. In addition, the majority of neuroblastoma cell lines harbor activating mutation in the MAPK cascade [9]. Furthermore, loss or reduced expression of *NF1*, a negative regulator of RAS, is also implicated in the pathogenesis of NB and associated with poor clinical outcome [40]. Aside from the endogenously dysregulated activation of the MAPK signaling cascade, growth factor-induced intracellular downstream signaling converge on the MAPK cascade, and are essential for tumor maintenance and progression. All of these observations highlight the significance of modulating the MAPK signaling axis for the treatment of NB. Our results showed that agerafenib significantly abrogated the activation of ERK MAPK signaling pathway.

Notably, compared with melanoma or thyroid cancer, *BRAF* mutations are rare in NB and are identified in only 1% of cases [41]. One major concern of using RAF inhibitors in tumors bearing wild type *BRAF* or oncogenic *RAS* mutations is paradoxical activation of the RAF downstream effectors MEK and ERK. This phenomenon is attributed to either the selective BRAF inhibitor-induced relief of the wild type RAF

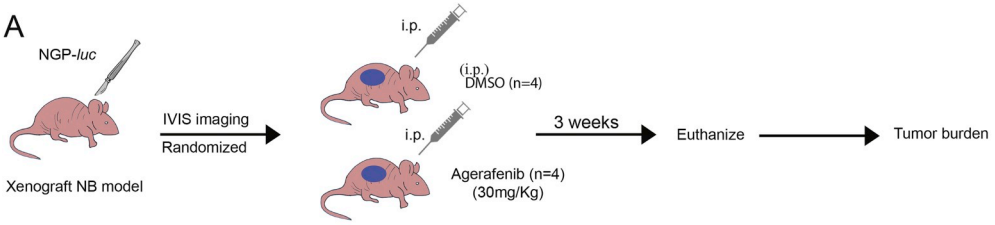

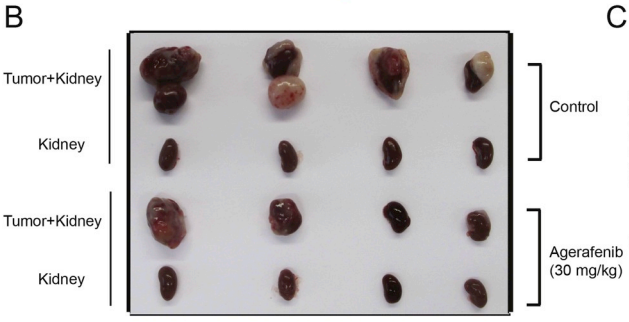

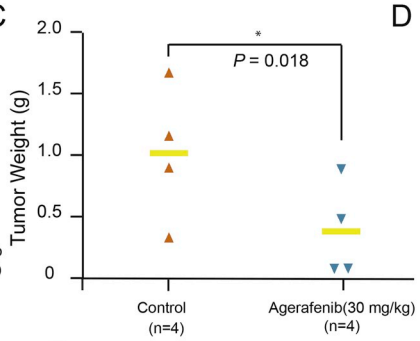

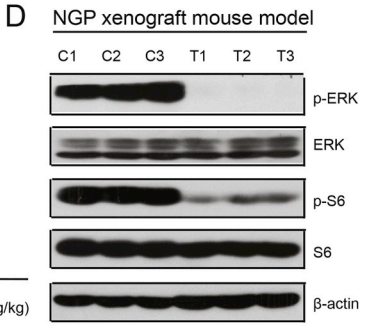

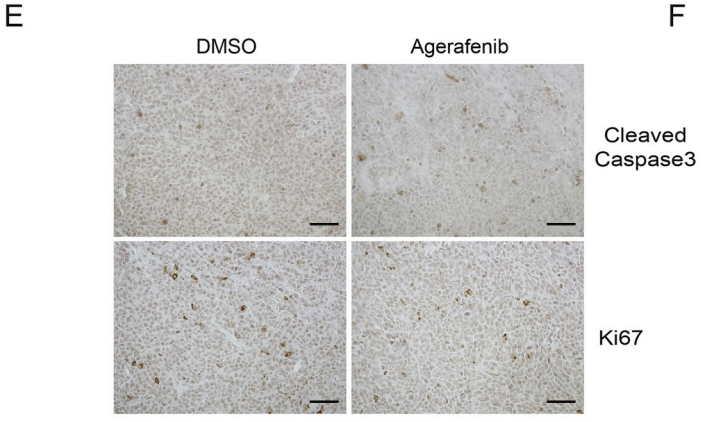

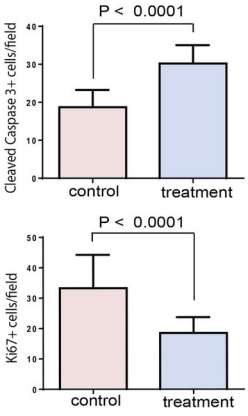

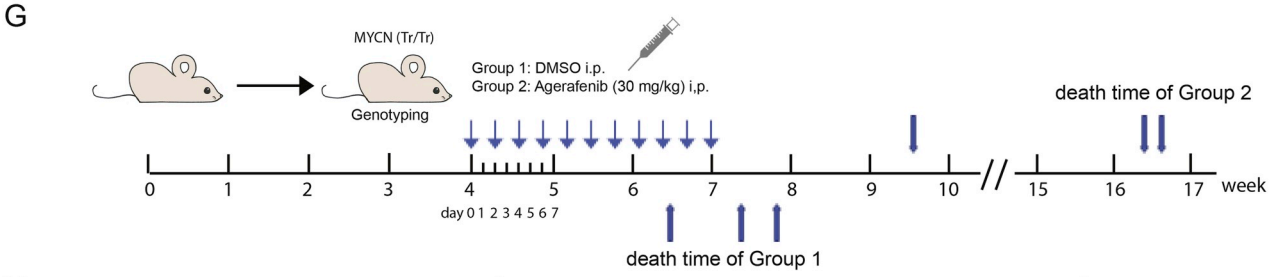

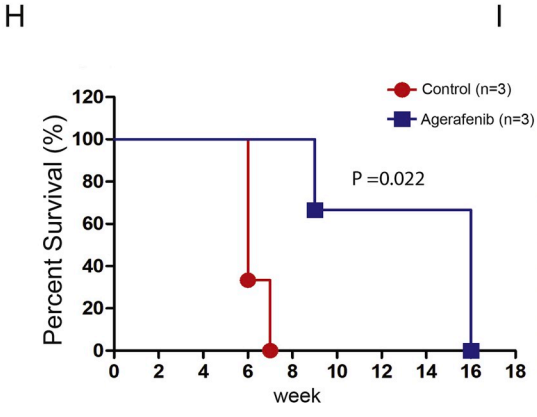

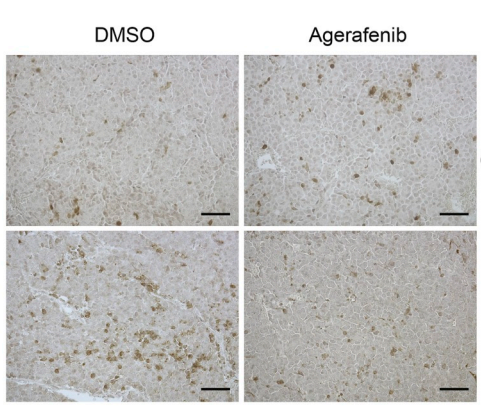

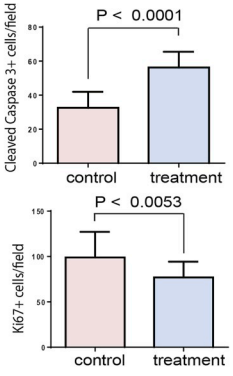

(caption on next page)

Fig. 5. Agerafenib inhibits tumor growth in a xenograft NB mouse model and prolongs survival in TH-*MYCN* transgenic NB mouse model. (A) Treatment strategy of the xenograft NB mouse model. (B) Photos of NGP xenografted tumors and corresponding kidney controls from the DMSO control group and the agerafenib treated group (30 mg/kg) were taken at the end of treatment (21 days). (C) NGP-derived individual final tumor weight values were plotted for the control (N = 4) and the agerafenib treated group (N = 4). *, P < 0.05 (Student's *t*-test, two tailed). (D) NGP-luciferase xenograft mouse bearing tumors were treated with 30 mg/kg agerafenib or an equal volume of DMSO by i.p. injection daily for 3 days. Then tumors were harvested and subjected to SDS-PAGE, and then immunoblotted with the antibodies indicated. (E) Immunohistochemistry staining of nuclear Ki-67 and cleaved caspase-3 on tumor sections from NGP xenograft NB mouse model after the treatment of agerafenib or DMSO control. (F) Quantification of cleaved caspase-3 and Ki67 of E (positive cell per high-power field). (G) Treatment strategy of the TH-*MYCN* transgenic NB mouse model. (H) Survival rate of TH-*MYCN* transgenic mice treated with agerafenib. Statistical analysis was performed by generalized Wilcoxon test. P = 0.022 compared with DMSO control and agerafenib. (I) Immunohistochemistry staining of nuclear Ki-67 and cleaved caspase-3 on tumor sections from TH-*MYCN* transgenic mouse model after the treatment of agerafenib or DMSO control. (J) Quantification of cleaved caspase-3 and Ki67 of I (positive cell per high-power field).

auto-inhibitory loop or the transactivation of RAF homodimers or heterodimers [18,42–44]. One potential mechanistic approach to preventing the paradoxical activation of the MAPK pathway while maintaining or improving efficacy of RAF inhibitors is the use of a pan-RAF inhibitor. Pan-RAF inhibition would block BRAF and CRAF kinases simultaneously, halting the activation of the downstream effectors MEK and ERK [42]. In this study, the novel pan-RAF small molecular inhibitor, agerafenib, significantly inhibited the ERK MAPK signaling cascade, and there was no paradoxical activation of ERK or S6 kinases observed in NB cell lines harboring wild type BRAF and CRAF, or RAS mutation. Our results show that agerafenib could effectively inhibit the ERK MAPK activation, making it a promising therapeutic agent to treat NB.

Our results showed that agerafenib significantly suppressed the NB cell proliferation and anchorage-independent growth. The inhibitory effect and the sensitivity of the tested cell lines to agerafenib were consistent with the change of ERK phosphorylation level. There was no accelerated cell proliferation observed post-agerafenib treatment, which presents further evidence that agerafenib prevents the selective RAF inhibitor-induced ERK MAPK activation. In addition, the potency of agerafenib had no statistically significant correlation with *MYCN* amplification status, allowing both *MYCN* amplified and non-amplified tumors to gain clinical benefit. In two typically refractory, chemo-resistant NB cell lines (SK–N-BE(2), SK-N-AS), agerafenib significantly enhanced the doxorubicin-induced apoptosis, suggesting that combined treatment with the chemotherapeutic agent represents a promising option for therapy-resistant or refractory NB patients.

In our study, two $RAS^{mut}/BRAF^{WT}$ cell lines, LAN-6 ($KRAS^{G12C}$) and SK-N-AS ($NRAS^{Q61K}$), showed different responses to agerafenib. The reason for this disparity may lie in the intrinsic gene expression profile. In previous studies, *NRAS* statuses were shown to be implicated in the resistance to MAPK signaling inhibition [45,46]. NRAS isoform 2 has been shown to play a role in RAF inhibitor resistance by facilitating alternative survival signaling through the PI3K pathway in the presence of MAPK pathway inhibition. However, agerafenib treatment had no inhibitory effect on the phosphorylation level of AKT in the treated *NRAS* mutant NB cell line SK-N-AS, as shown in Fig.S2C, suggesting that agerafenib had no effect on the alternative activation of the PI3K pathway. The disparity of the sensitivity of different *RAS* mutant cell lines to MAPK signaling inhibition was also found in two other non-NB cell lines, the lung cancer cell (A549, $KRAS^{G12S}$) and the breast cancer cell (MDA-MB-231, $KRAS^{G13D}$), although both of the cell lines showed relatively higher sensitivity to agerafenib when compared with SK-N-AS (Fig.S3F). However, when they were treated with trametinib, they showed significantly different responsiveness. There was nearly a 680-fold difference of the IC_{50} values between the two cell lines after treatment with trametinib (Fig.S3G). Therefore, the exact mechanism of this phenomenon needs further investigation.

It is also worth noticing that the insensitive cell line (SK–N-AS, RAS^{mut}) in our study showed a high responsiveness to MEK inhibition in another study, while the cell line (NGP, RAS^{WT}) that was resistant to MEK inhibition turned out to be sensitive to agerafenib [47]. Although we don't know the exact mechanism for this phenomenon, it implies that the combination of agerafenib and MEK inhibition may produce a vertical synergistic effect on tumors bearing RAS mutations. This therapeutic concept was also supported by the data from a newly published study, in which the authors found that MEK inhibitors could re-wire RAS mutant tumors pharmacologically and sensitize tumors to RAF kinase inhibition [48].

Based on the cell proliferation inhibition results and the synergism assay in our *in vitro* experiments, we evaluated the *in vivo* antitumor efficacy and tolerability of agerafenib in two NB mouse models. NB mouse models could faithfully recapitulate the histological and genetic features of aggressive tumors and, therefore, are well suited for screening the clinical efficacy and safety of potential new drugs [49,50]. The potent tumor regression, prolonged lifespan, and favorable toxicity profile observed in the two NB mouse models further demonstrated the therapeutic efficacy of agerafenib. Agerafenib has shown a tolerable safety profile in adults with advanced or metastatic solid tumors. The majority of the treatment-related adverse events (AEs) were ≤ Grade 2. The most commonly observed Grade 3 AEs (> 5%) were rashes (10%), hypophosphatemia (7%), and elevated ALT (7%) [51].

In conclusion, to the best of our knowledge, this is the first study to evaluate the anti-tumor effect of agerafenib on NB. Although our preclinical studies are promising, the therapeutic mechanisms of agerafenib remain to be fully explored. Based on our preclinical *in vitro* and *in vivo* data, treatment with agerafenib or its combination with traditional chemotherapy may represent a promising approach for treating high-risk NB patients.

Conflicts of interest

The authors declare no conflicts of interest.

Grant support

This work was supported by the Dan L Duncan Comprehensive Cancer Center (DLDCC) Pilot Award (to J.H.F.) and the Elsa U. Pardee Foundation Award (to J.H.F.).

Acknowledgement

The authors would like to thank Dr. Deyong Jia at University of Washington for valuable discussions, suggestions, and for revising the paper, and thank Andrew V. Yang for critical reading of the manuscript. This work is dedicated to all the children suffering from neuroblastoma who inspire us to work hard to find a cure.

Appendix A. Supplementary data

Supplementary data to this article can be found online at https://doi.org/10.1016/j.canlet.2019.05.011.

References

[1] G.M. Brodeur, Neuroblastoma: biological insights into a clinical enigma, Nat. Rev. Canc. 3 (2003) 203–216.
[2] R. David, N. Lamki, S. Fan, E.B. Singleton, F. Eftekhari, A. Shirkhoda, R. Kumar, J.E. Madewell, The many faces of neuroblastoma, Radiographics 9 (1989) 859–882.
[3] P. Kaatsch, Epidemiology of childhood cancer, Cancer Treat Rev. 36 (2010) 277–285.
[4] M. Schwab, F. Westermann, B. Hero, F. Berthold, Neuroblastoma: biology and molecular and chromosomal pathology, Lancet Oncol. 4 (2003) 472–480.
[5] N.R. Pinto, M.A. Applebaum, S.L. Volchenboum, K.K. Matthay, W.B. London, P.F. Ambros, A. Nakagawara, F. Berthold, G. Schleiermacher, J.R. Park, D. Valteau-Couanet, A.D. Pearson, S.L. Cohn, Advances in risk classification and treatment strategies for neuroblastoma, J. Clin. Oncol. 33 (2015) 3008–3017.
[6] K.K. Matthay, J.G. Villablanca, R.C. Seeger, D.O. Stram, R.E. Harris, N.K. Ramsay, P. Swift, H. Shimada, C.T. Black, G.M. Brodeur, R.B. Gerbing, C.P. Reynolds, Treatment of high-risk neuroblastoma with intensive chemotherapy, radiotherapy, autologous bone marrow transplantation, and 13-cis-retinoic acid. Children's Cancer Group, N. Engl. J. Med. 341 (1999) 1165–1173.
[7] K.A. Cole, J.M. Maris, New strategies in refractory and recurrent neuroblastoma: translational opportunities to impact patient outcome, Clin. Cancer Res. 18 (2012) 2423–2428.
[8] W. Kolch, Meaningful relationships: the regulation of the Ras/Raf/MEK/ERK pathway by protein interactions, Biochem. J. 351 (2000) 289–305.
[9] T.F. Eleveld, D.A. Oldridge, V. Bernard, J. Koster, L. Colmet Daage, S.J. Diskin, L. Schild, N.B. Bentahar, A. Bellini, M. Chicard, E. Lapouble, V. Combaret, P. Legoix-Ne, J. Michon, T.J. Pugh, L.S. Hart, J. Rader, E.F. Attiyeh, J.S. Wei, S. Zhang, A. Naranjo, J.M. Gastier-Foster, M.D. Hogarty, S. Asgharzadeh, M.A. Smith, J.M. Guidry Auvil, T.B. Watkins, D.A. Zwijnenburg, M.E. Ebus, P. van Sluis, A. Hakkert, E. van Wezel, C.E. van der Schoot, E.M. Westerhout, J.H. Schulte, G.A. Tytgat, M.E. Dolman, I. Janoueix-Lerosey, D.S. Gerhard, H.N. Caron, O. Delattre, J. Khan, R. Versteeg, G. Schleiermacher, J.J. Molenaar, J.M. Maris, Relapsed neuroblastomas show frequent RAS-MAPK pathway mutations, Nat. Genet. 47 (2015) 864–871.
[10] L. Lopez-Delisle, C. Pierre-Eugene, C. Louis-Brennetot, D. Surdez, V. Raynal, S. Baulande, V. Boeva, S. Grossetete-Lalami, V. Combaret, M. Peuchmaur, O. Delattre, I. Janoueix-Lerosey, Activated ALK signals through the ERK-ETV5-RET pathway to drive neuroblastoma oncogenesis, Oncogene 37 (2018) 1417–1429.
[11] R. Ho, J.E. Minturn, T. Hishiki, H. Zhao, Q. Wang, A. Cnaan, J. Maris, A.E. Evans, G.M. Brodeur, Proliferation of human neuroblastomas mediated by the epidermal growth factor receptor, Cancer Res. 65 (2005) 9868–9875.
[12] J.I. Johnsen, C. Dyberg, S. Fransson, M. Wickstrom, Molecular mechanisms and therapeutic targets in neuroblastoma, Pharmacol. Res. 131 (2018) 164–176.
[13] I. Lambertz, C. Kumps, S. Claeys, S. Lindner, A. Beckers, E. Janssens, D.R. Carter, A. Cazes, B.B. Cheung, M. De Mariano, A. De Bondt, S. De Brouwer, O. Delattre, J. Gibbons, I. Janoueix-Lerosey, G. Laureys, C. Liang, G.M. Marchall, M. Porcu, J. Takita, D.C. Trujillo, I. Van Den Wyngaert, N. Van Roy, A. Van Goethem, T. Van Maerken, P. Zabrocki, J. Cools, J.H. Schulte, J. Vialard, F. Speleman, K. De Preter, Upregulation of MAPK negative feedback regulators and RET in mutant ALK neuroblastoma: implications for targeted treatment, Clin. Cancer Res. 21 (2015) 3327–3339.
[14] F. McPhillips, P. Mullen, K.G. MacLeod, J.M. Sewell, B.P. Monia, D.A. Cameron, J.F. Smyth, S.P. Langdon, Raf-1 is the predominant Raf isoform that mediates growth factor-stimulated growth in ovarian cancer cells, Carcinogenesis 27 (2006) 729–739.
[15] B. Agianian, E. Gavathiotis, Current insights of BRAF inhibitors in cancer, J. Med. Chem. 61 (2018) 5775–5793.
[16] S. An, Y. Yang, R. Ward, Y. Liu, X.X. Guo, T.R. Xu, A-Raf: a new star of the family of raf kinases, Crit. Rev. Biochem. Mol. Biol. 50 (2015) 520–531.
[17] M. Xing, BRAF mutation in thyroid cancer, Endocr. Relat. Cancer 12 (2005) 245–262.
[18] P.A. Ascierto, J.M. Kirkwood, J.J. Grob, E. Simeone, A.M. Grimaldi, M. Maio, G. Palmieri, A. Testori, F.M. Marincola, N. Mozzillo, The role of BRAF V600 mutation in melanoma, J. Transl. Med. 10 (2012) 85.
[19] C.N. Clarke, E.S. Kopetz, BRAF mutant colorectal cancer as a distinct subset of colorectal cancer: clinical characteristics, clinical behavior, and response to targeted therapies, J. Gastrointest. Oncol. 6 (2015) 660–667.
[20] W. Pao, N. Girard, New driver mutations in non-small-cell lung cancer, Lancet Oncol. 12 (2011) 175–180.
[21] H. Davies, G.R. Bignell, C. Cox, P. Stephens, S. Edkins, S. Clegg, J. Teague, H. Woffendin, M.J. Garnett, W. Bottomley, N. Davis, E. Dicks, R. Ewing, Y. Floyd, K. Gray, S. Hall, R. Hawes, J. Hughes, V. Kosmidou, A. Menzies, C. Mould, A. Parker, C. Stevens, S. Watt, S. Hooper, R. Wilson, H. Jayatilake, B.A. Gusterson, C. Cooper, J. Shipley, D. Hargrave, K. Pritchard-Jones, N. Maitland, G. Chenevix-Trench, G.J. Riggins, D.D. Bigner, G. Palmieri, A. Cossu, A. Flanagan, A. Nicholson, J.W. Ho, S.Y. Leung, S.T. Yuen, B.L. Weber, H.F. Seigler, T.L. Darrow, H. Paterson, R. Marais, C.J. Marshall, R. Wooster, M.R. Stratton, P.A. Futreal, Mutations of the BRAF gene in human cancer, Nature 417 (2002) 949–954.
[22] Y.H. Hwang, J.Y. Choi, S. Kim, E.S. Chung, T. Kim, S.S. Koh, B. Lee, S.H. Bae, J. Kim, Y.M. Park, Over-expression of c-raf-1 proto-oncogene in liver cirrhosis and hepatocellular carcinoma, Hepatol. Res. 29 (2004) 113–121.
[23] Z. Liu, Y. Liu, L. Li, Z. Xu, B. Bi, Y. Wang, J.Y. Li, MiR-7-5p is frequently down-regulated in glioblastoma microvasculature and inhibits vascular endothelial cell proliferation by targeting RAF1, Tumour Biol 35 (2014) 10177–10184.
[24] F. Wang, C. Jiang, Q. Sun, F. Yan, L. Wang, Z. Fu, T. Liu, F. Hu, miR-195 is a key regulator of Raf1 in thyroid cancer, OncoTargets Ther. 8 (2015) 3021–3028.
[25] Y. Huang, X.X. Guo, B. Han, X.M. Zhang, S. An, X.Y. Zhang, Y. Yang, Y. Liu, Q. Hao, T.R. Xu, Decoding the full picture of Raf1 function based on its interacting proteins, Oncotarget 8 (2017) 68329–68337.
[26] W. Kolch, G. Heidecker, P. Lloyd, U.R. Rapp, Raf-1 protein kinase is required for growth of induced NIH/3T3 cells, Nature 349 (1991) 426–428.
[27] Z.H. Xu, J.B. Hang, J.A. Hu, B.L. Gao, RAF1-MEK1-ERK/AKT axis may confer NSCLC cell lines resistance to erlotinib, Int. J. Clin. Exp. Pathol. 6 (2013) 1493–1504.
[28] Z. Xiao, N. Ding, G. Xiao, S. Wang, Y. Wu, L. Tang, Reversal of multidrug resistance by gefitinib via RAF1/ERK pathway in pancreatic cancer cell line, Anat. Rec. 295 (2012) 2122–2128.
[29] C. Montagut, J. Settleman, Targeting the RAF-MEK-ERK pathway in cancer therapy, Cancer Lett. 283 (2009) 125–134.
[30] S. Wilhelm, C. Carter, M. Lynch, T. Lowinger, J. Dumas, R.A. Smith, B. Schwartz, R. Simantov, S. Kelley, Discovery and development of sorafenib: a multikinase inhibitor for treating cancer, Nat. Rev. Drug Discov. 5 (2006) 835–844.
[31] Z. Karoulia, E. Gavathiotis, P.I. Poulikakos, New perspectives for targeting RAF kinase in human cancer, Nat. Rev. Canc. 17 (2017) 676–691.
[32] J. James, B. Ruggeri, R.C. Armstrong, M.W. Rowbottom, S. Jones-Bolin, R.N. Gunawardane, P. Dobrzanski, M.F. Gardner, H. Zhao, M.D. Cramer, K. Hunter, R.R. Nepomuceno, M. Cheng, D. Gitnick, M. Yazdanian, D.E. Insko, M.A. Ator, J.L. Apuy, R. Faraoni, B.D. Dorsey, M. Williams, S.S. Bhagwat, M.W. Holladay, CEP-32496: a novel orally active BRAF(V600E) inhibitor with selective cellular and in vivo antitumor activity, Mol. Cancer Ther. 11 (2012) 930–941.
[33] H. Li, Z. Chen, T. Hu, L. Wang, Y. Yu, Y. Zhao, W. Sun, S. Guan, J.C. Pang, S.E. Woodfield, Q. Liu, J. Yang, Novel proteasome inhibitor ixazomib sensitizes neuroblastoma cells to doxorubicin treatment, Sci. Rep. 6 (2016) 34397.
[34] H. Zhang, J. Dou, Y. Yu, Y. Zhao, Y. Fan, J. Cheng, X. Xu, W. Liu, S. Guan, Z. Chen, Y. shi, R. Patel, S.A. Vasudevan, P.E. Zage, H. Zhang, J.G. Nuchtern, E.S. Kim, S. Fu, J. Yang, mTOR ATP-competitive inhibitor INK128 inhibits neuroblastoma growth via blocking mTORC signaling, Apoptosis 20 (2015) 50–62.
[35] J. Lu, S. Guan, Y. Zhao, Y. Yu, S.E. Woodfield, H. Zhang, K.L. Yang, S. Bieerkehazhi, L. Qi, X. Li, J. Gu, X. Xu, J. Jin, J.A. Muscal, T. Yang, G.T. Xu, J. Yang, The second-generation ALK inhibitor alectinib effectively induces apoptosis in human neuroblastoma cells and inhibits tumor growth in a TH-MYCN transgenic neuroblastoma mouse model, Cancer Lett. 400 (2017) 61–68.
[36] T.C. Chou, Drug combination studies and their synergy quantification using the Chou-Talalay method, Cancer Res. 70 (2010) 440–446.
[37] Y. Wang, L. Wang, S. Guan, W. Cao, H. Wang, Z. Chen, Y. Zhao, Y. Yu, H. Zhang, J.C. Pang, S.L. Huang, Y. Akiyama, Y. Yang, W. Sun, X. Xu, Y. Shi, H. Zhang, E.S. Kim, J.A. Muscal, F. Lu, J. Yang, Novel ALK inhibitor AZD3463 inhibits neuroblastoma growth by overcoming crizotinib resistance and inducing apoptosis, Sci. Rep. 6 (2016) 19423.
[38] M. Huang, W.A. Weiss, Neuroblastoma and MYCN, Cold Spring Harb Perspect Med 3 (2013) a014415.
[39] G. Umapathy, J. Guan, D.E. Gustafsson, N. Javanmardi, D. Cervantes-Madrid, A. Djos, T. Martinsson, R.H. Palmer, B. Hallberg, MEK inhibitor trametinib does not prevent the growth of anaplastic lymphoma kinase (ALK)-addicted neuroblastomas, Sci. Signal. 10 (2017).
[40] M. Holzel, S. Huang, J. Koster, I. Ora, A. Lakeman, H. Caron, W. Nijkamp, J. Xie, T. Callens, S. Asgharzadeh, R.C. Seeger, L. Messiaen, R. Versteeg, R. Bernards, NF1 is a tumor suppressor in neuroblastoma that determines retinoic acid response and disease outcome, Cell 142 (2010) 218–229.
[41] N. Shukla, N. Ameur, I. Yilmaz, K. Nafa, C.Y. Lau, A. Marchetti, L. Borsu, F.G. Barr, M. Ladanyi, Oncogene mutation profiling of pediatric solid tumors reveals significant subsets of embryonal rhabdomyosarcoma and neuroblastoma with mutated genes in growth signaling pathways, Clin. Cancer Res. 18 (2012) 748–757.
[42] S.J. Heidorn, C. Milagre, S. Whittaker, A. Nourry, I. Niculescu-Duvas, N. Dhomen, J. Hussain, J.S. Reis-Filho, C.J. Springer, C. Pritchard, R. Marais, Kinase-dead BRAF and oncogenic RAS cooperate to drive tumor progression through CRAF, Cell 140 (2010) 209–221.
[43] G. Hatzivassiliou, K. Song, I. Yen, B.J. Brandhuber, D.J. Anderson, R. Alvarado, M.J. Ludlam, D. Stokoe, S.L. Gloor, G. Vigers, T. Morales, I. Aliagas, B. Liu, S. Sideris, K.P. Hoeflich, B.S. Jaiswal, S. Seshagiri, H. Koeppen, M. Belvin, L.S. Friedman, S. Malek, RAF inhibitors prime wild-type RAF to activate the MAPK pathway and enhance growth, Nature 464 (2010) 431–435.
[44] G.S. Falchook, M. Millward, D. Hong, A. Naing, S. Piha-Paul, S.G. Waguespack, M.E. Cabanillas, S.I. Sherman, B. Ma, M. Curtis, V. Goodman, R. Kurzrock, BRAF inhibitor dabrafenib in patients with metastatic BRAF-mutant thyroid cancer, Thyroid 25 (2015) 71–77.
[45] M.C. Duggan, A.R. Stiff, M. Bainazar, K. Regan, G.N. Olaverria Salavaggione, S. Maharry, J.S. Blachly, M. Krischak, C.J. Walker, N. Latchana, S. Tridandapani, A. de la Chapelle, A.K. Eisfeld, W.E. Carson 3rd, Identification of NRAS isoform 2 overexpression as a mechanism facilitating BRAF inhibitor resistance in malignant melanoma, Proc. Natl. Acad. Sci. U. S. A. 114 (2017) 9629–9634.
[46] Z. Wang, Y. Li, E.T. Liu, Q. Yu, Susceptibility to cell death induced by blockade of MAPK pathway in human colorectal cancer cells carrying Ras mutations is dependent on p53 status, Biochem. Biophys. Res. Commun. 322 (2004) 609–613.
[47] S.E. Woodfield, L. Zhang, K.A. Scorsone, Y. Liu, P.E. Zage, Binimetinib inhibits MEK and is effective against neuroblastoma tumor cells with low NF1 expression, BMC Canc. 16 (2016) 172.
[48] I. Yen, F. Shanahan, M. Merchant, C. Orr, T. Hunsaker, M. Durk, H. La, X. Zhang, S.E. Martin, E. Lin, J. Chan, Y. Yu, D. Amin, R.M. Neve, A. Gustafson, A. Venkatanarayan, S.A. Foster, J. Rudolph, C. Klijn, S. Malek, Pharmacological induction of RAS-GTP confers RAF inhibitor sensitivity in KRAS mutant tumors,

Cancer Cell 34 (2018) 611–625 e617.
[49] C. Khanna, J.J. Jaboin, E. Drakos, M. Tsokos, C.J. Thiele, Biologically relevant orthotopic neuroblastoma xenograft models: primary adrenal tumor growth and spontaneous distant metastasis, In Vivo 16 (2002) 77–85.
[50] N. Braekeveldt, C. Wigerup, D. Gisselsson, S. Mohlin, M. Merselius, S. Beckman, T. Jonson, A. Borjesson, T. Backman, I. Tadeo, A.P. Berbegall, I. Ora, S. Navarro, R. Noguera, S. Pahlman, D. Bexell, Neuroblastoma patient-derived orthotopic xenografts retain metastatic patterns and geno- and phenotypes of patient tumours, Int. J. Cancer 136 (2015) E252–E261.
[51] S.V.L. Alexander Drilon, Robert Doebele, Cristina Rodriguez, A phase 1b study of RXDX-105, a VEGFR-sparing potent RET inhibitor, RETi-Naïve Patients with RET Fusion-Positive NSCLC Annals of Oncology, vol. 28, 2017.